Chin.J.Geochem.(2014)33:374–381
DOI: 10.1007/s11631-014-0700-4

Electrochemical behavior of pyrite in acidic solution with different concentrations of NaCl

LIN Sen[1,2], LIU Qingyou[1], and LI Heping[1*]

[1] *Laboratory for High Temperature & High Pressure Study of the Earth's Interior, Institute of Geochemistry, Chinese Academy of Sciences, Guiyang 550002, China*

[2] *University of Chinese Academy of Sciences, Beijing 100049, China*

[*] *Corresponding author, E-mail: liheping@vip.skleg.cn*

Received December 1, 2013; accepted January 12, 2014

Abstract The role of chloride ions in metal sulfides leaching has been well established by researchers, the complexation of chloride ions was considered to be the main effect of chloride ions. In this work, the complexation of chloride ions was neglected by addition of EDTA, a strong complexing agent. In this way, further study was conducted on the effect of chloride ions. The increase of chloride ions concentration from 0 to 2 mol/L, decreased the open circuit potential of pyrite from 264 to 91 mV. Unless otherwise stated, all potentials in this paper are based on the potential of saturated calomel electrode. At 600 mV, the increase of chloride ions concentration acceleraed pyrite oxidation; at 800 and 1000 mV, however, the increase of chloride ions concentration lowered pyrite oxidation rate, and the proportion of elemental sulfur was also decreased with increasing chloride ions concentration; when chloride ions concentration increased from 0 to 2 mol/L, the proportion of elemental sulfur decreased from 32% to 28.4% at 800 mV, and 7.1% to 2.4% at 1000 mV.

Key words pyrite; anodic oxidation; NaCl; EDTA; adsorption

1 Introduction

The oxidation of pyrite has attracted the attention of researchers for its importance in nature and hydrometallurgy industry. Pyrite is widely present in the Earth's crust, especially seabed sediments, and the oxidation of pyrite is related to the circulation of S and Fe in nature. In hydrometallurgy, leaching (Dutrizac, 1992; Antonijevic et al., 1997) and flotation (Boulton et al., 2003; Chandra and Gerson, 2009) are effective methods for separating pyrite from other minerals, based on the oxidation of pyrite. The acid mine drainage (AMD) caused by oxidation of abandoned pyrite and other sulfides has become a pollution problem all over the world (Balci et al., 2007; Webera et al., 2004; Baker and Banfield, 2003).

Researches showed that the oxidation of pyrite was a multistep electrochemical process, which began from the interaction of water molecules and the S_2^{2-} ions on pyrite surface lattice (Rimstidt and Vaughan, 2003; Kelsall et al., 1999; Descostes et al., 2004). The results of *in-situ* Raman analysis and Fourier transform infrared spectroscopy revealed that intermediate products, such as $S_2O_3^{2-}$, SO_3^{2-}, and $S_xO_6^{2-}$ (Kelsall et al., 1999; Lehmann et al., 2000; Chernyshova, 2003), were generated but finally, the sulfur mainly existed in the form of SO_4^{2-} and elemental sulfur. In addition, researchers found that the elemental sulfur would be adsorbed onto the surface, and was responsible for the passivation of pyrite (Lin and Say, 1999; Long and Dixon, 2004), while the proportion of elemental sulfur in oxidation products decreased with increasing applied potential (Biegler and Swift, 1979; Flatt and Woods, 1995). The anode half-reaction can be expressed as follows (Biegler and Swift, 1979),

$$FeS_2+(8-4x)\,H_2O \rightarrow Fe^{3+}+xS+(2-x)\,SO_4^{2-} +(16-8x)\,H^{+}+(15-6x)e^{-} \quad (1)$$

The oxidation of pyrite is greatly affected by solution environment. So far, there are reports on the effects of ferric ions (Moses et al., 1987; Williamson

and Rimstidt, 1994; Liu et al., 2011), dissolved oxygen (Lowson, 1982), pH (Bonnissel-Gissinger et al., 1998), other inorganic ions (Chandra and Gerson, 2011), and temperature (Mckibben and Barnes, 1986). Chloride ion, an aggressive ion, usually appears in the oxidation of pyrite, both in nature and in hydrometallurgy industry. The role of chloride ions was also investigated, especially in sulfide leaching researches (Senanayake, 2009). They reported that chloride ion speeded up the corrosion of the mineral in two pathways, firstly, chloride ion would combine with metal ions and resulted in increased solubility of oxidation products (Xiong and Guo, 2011); secondly, chloride ion would depress the passivation of the surface (Carneiro and Leao, 2007). Chloride ion is a strong Lewis base, it often plays a complex role in the corrosion of materials. However, the effects of chloride ion in pyrite oxidation besides its complexation and depassivation were rarely reported, neither the effects at different potential areas were discussed.

In this work, the effects of chloride ion in pyrite oxidation were studied. EDTA was added to achieve two effects, (1) to neglect the complexation of chloride ions by complexing competition, and (2) to lower the potential of the redox couple Fe(III)/Fe(II), making iron in the products exist only in the valence of Fe(III). We conducted research on the open circuit potential (OCP), anodic polarization curve, cyclic voltammetric (CV) curve, chronoamperometric curve of pyrite at different potentials in solutions with different concentrations of chloride ions. The purpose of this study was to identify the effects of chloride ion concentrations on the OCP of pyrite and the kinetic parameter of the anodic process, as well as those on the pyrite oxidation rate and the proportion of elemental sulfur in oxidation products at different potential areas.

2 Materials and methods

All electrochemical experiments were performed with a standard three-electrode system. The anode chamber was separated from the cathode chamber with an anion exchange membrane. The reference electrode was a saturated calomel electrode (SCE, 245.8 mV versus SHE at 25℃). The counter electrode was a round platinum gauze electrode with a diameter of 2.0 cm, and the working electrode was made of natural pyrite from Longsheng, Guangxi Province, China. Powder X-ray diffraction and electron probe analysis showed that more than 99.5% of the working electrode was FeS_2 and the impurities were mainly quartz. The pyrite was first cut and polished into a cylinder with 2.0 cm in height and 1.0 cm in diameter, then one end was connected to a copper conductor with silver powder conductive adhesive. Next, epoxy resin was used to seal the electrode, leaving the other end exposed. The apparent area of the working electrode was 0.785 cm^2; before each experiment, we used 1000 and 2000-mesh silicon carbide abrasive papers and 0.5-μm diamond paste to polish the electrode surface. Finally, the electrode was washed with ethanol and ultrapure water.

The electrolyte used in the experiment was NaCl solution at concentrations of 0.0, 0.5, 1.0, 1.5, and 2.0 mol/L; 0.1 mol/L $NaClO_4$ was added as the supporting electrolyte, together with 1×10^{-3} mol/L EDTA. The original pH of the solution was adjusted to 3.00 by using $HClO_4$. Before every test, nitrogen was introduced into the electrolyte for 30 minutes to remove the dissolved oxygen in the solution; when the test began, nitrogen was kept on above the liquid level to keep air out. The electrolyser was placed in a thermostatic water bath equipped with a magnetic agitator; the reaction temperature was set at 25℃, and the magnetic agitator was started when necessary. The whole reaction device was placed in an electromagnetic shielding box to eliminate the interference of external electromagnetic fields. A Princeton 2263 electrochemical workstation connected to a computer was used for the measurements with the aid of the Powersuite software; atomic absorption spectroscopy (AAS) was used to determine the content of iron in the electrolyte. Analytical reagents and ultrapure water were used in the experiments.

3 Results and discussion

3.1 Open circuit potential

The influence of NaCl concentration on OCP of pyrite was measured. A close relationship between this potential and electrode surface condition was previously reported (Wei and Osseoasare, 1996; Cabral and Ignatiadis, 2001). Differences in electrode pretreatment resulted in a significant variation in OCP of pyrite in previous studies. Antonijevic et al. (2005) suggested that OCP increased with increasing concentrations of chloride ions in electrolyte. While, Moslemi et al. (2011) pointed out that the increas concentration of chloride ions decreased this potential. The conflict might originate from the difference in pyrite pretreatment.

In this study, to preclude the uncertainties derived from the difference in each pyrite electrode polishing process, the pyrite electrode was polished and washed only once, then right amount of deoxidized NaCl crystals (dissolved in water and deoxygened with N_2, then dried in oxygen-free environment) was added to the initial electrolyte containing 0.1 mol/L $NaClO_4$ and 1×10^{-3} mol/L EDTA (pH 3.00) every 2 h to obtain the chloride ion concentration in the electrolyte at 0.0,

0.5, 1.0, 1.5, and 2.0 mol/L. As shown in Fig. 1, the OCP of pyrite increased with time and reached quasi-steady state in approximately 20 minutes in the absence of NaCl, at a value of about 264 mV, where the quasi-steady state was defined here as a change of lower than 2 mV·min^{-1}. However, the OCP significantly decreased with the addition of NaCl, and reached another quasi-steady state at 207 mV in approximately 30 minutes. Afterward, each addition of NaCl would produce a decrease in OCP, causing the same change in potentialtime curve. The decrease in OCP by the first addition of 0.5 mol/L NaCl was 57 mV, while, this value went down gradually in the following addition of NaCl, e.g. 45 mV in the second, and 23 mV in the last addition.

OCP of pyrite is a mixed potential fixed by the redox of pyrite and species in the electrolyte. The redox potential (Eh) of the electrolyte was measured by a platinum electrode, and it changed from 196 mV to 172 mV when NaCl concentration increased from 0 to 2 mol/L, only decreased at a scale of 24 mV. Thus, the fall in pyrite redox potential was the main reason for the decrease in OCP.

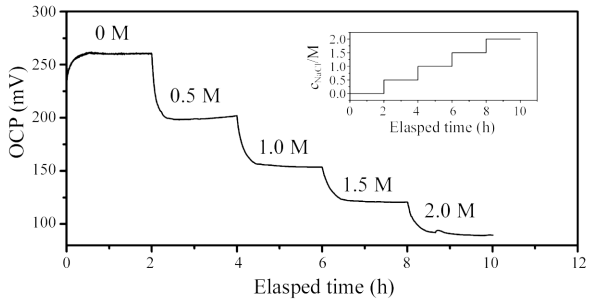

Fig. 1. The open circuit potential of pyrite as the NaCl concentration increasing at 0.5 mol/L every 2 hours, vs. SCE.

3.2 Anodic polarization study

Polarization curves of pyrite were measured with different NaCl concentrations (Fig. 2). The scanning rate was 1 mV/s.

The trend of the measured anodic polarization curves measured in this work was similar to the results measured by Antonijevic et al. (2005). Electrochemical parameters, such as corrosion potential (E_{corr}), anodic exchange current density ($j_{0,a}$), and anodic Tafel slope (β_a), were obtained from the anodic polarization curves (Table 1). With NaCl concentration increased from 0 to 2 mol/L, E_{corr} decreased from 264.5 to 91.6 mV, β_a decreased from 74.6 to 65.8 mV/decade, whereas $j_{0,a}$ of the electrode showed an opposite trend, increased from 6.1×10^{-5} to 9.0×10^{-4} mA·cm^{-2}.

The variation tendency of electrochemical kinetics parameters shows an agreed suggestion that pyrite is corroded faster with a higher NaCl concentration. Carneiro and Leao (2007) found that with chloride ions, a porous and somewhat crystalline sulfur layer formed on sulfide surface, instead of a tight passivated sulfur layer in absence of chloride ions. The change in morphology of elemental sulfur layer contributes to that pyrite is easy to be oxidized.

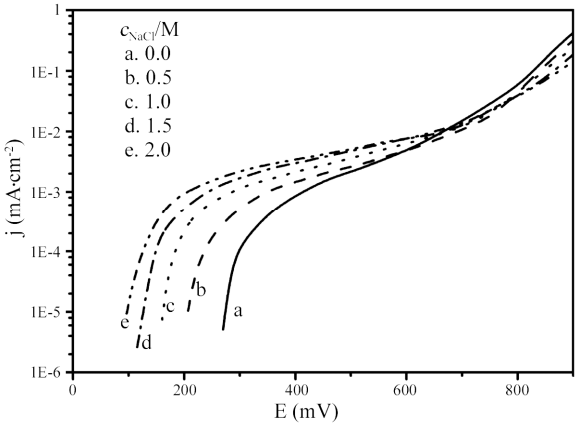

Fig. 2. Anodic branch of polarization curves of pyrite in electrolytes with different NaCl concentrations (scan rate 1 mV·s^{-1}, pH 3.00, vs. SCE).

3.3 Cyclic voltammetry study

Cyclic voltammetry was applied to study the electrochemical reaction of pyrite with different NaCl concentrations and the effect of EDTA. Fig. 3 showed the first two cycles of the cyclic voltammetric curve of pyrite in the electrolyte containing 2 mol/L NaCl and 0.1 mol/L $NaClO_4$, without EDTA. The potential range of each peak agreed well with literatures (Tao et al., 2003; Giannetti et al., 2001). Near -500 mV, a reduction peak, C_1, appeared in the second cycle but not presented in the first cycle, indicating that C_1 was generated due to the reduction of oxidation products produced in the first cycle of scanning. C_1 might be the reduction of elemental sulfur as follows,

$$S+2H^{+}+2e^{-}\rightarrow H_2S \quad (2)$$

This is consistent with the results measured by Tao et al. (2003) Another reduction peak, C_2, was generated by the reduction of pyrite near -650 mV in the first cycle, corresponding to the following reaction,

$$FeS_2+2e^{-}+2H^{+}\rightarrow FeS+H_2S \quad (3)$$

In the second cycle, due to the coating of elemental sulfur, C_2 shifted toward the negative direction for approximately 50 mV. FeS generated in Reaction (3) was then dissolved in the acidic environment:

$$FeS+2H^{+}\rightarrow Fe^{2+}+H_2S \quad (4)$$

As the scan went on from -800 to 800 mV, three oxidation peaks appeared, A_1, A_2, and A_3. The A_1 appeared near -100 mV, which was the oxidation peak of H_2S produced in Reactions (3) and (4) (Giannetti et al., 2001),

$$H_2S \rightarrow S+2H^+ +2e^- \quad (5)$$

The A_2, a weak oxidation peak, appeared near approximately 600 mV, which corresponded to the oxidation of ferrous ion at pyrite surface (Ahlberg and Broo, 1997),

$$Fe^{2+} \rightarrow Fe^{3+} + e^- \quad (6)$$

The oxidation of pyrite also began at this potential. The oxidation rate increased quickly with the rising scanning potential, resulted in the appearance of a sharp peak, A_3, which is related to Reaction (1). The scanning potential reversed at 800 mV, another weak reduction peak, C_3, appeared around 400 mV, which was the reversible peak of A_2, corresponding to the reduction of ferric ions (Ahlberg and Broo, 1997),

$$Fe^{3+}+e^- \rightarrow Fe^{2+} \quad (7)$$

Soluble ferric ions, ferrous ions, and hydrogen sulfide generated in scanning process diffused rapidly from the electrode surface to the electrolyte when stirred, so their concentrations were approximately zero near pyrite surface. Therefore, peaks A_1, A_2, and C_3 disappeared from the cyclic voltammetric curve (Fig. 4) when stirred. Stirring accelerated the redox of insoluble species by enhancing diffusion of reaction products, so peaks A_3 and C_2 were strengthened. However, the reduction peak of sulfur, C_1, decreased slightly, though stirring also accelerated the diffusion of the generated hydrogen sulfide. This might be due to the fact that elemental sulfur produced in pyrite oxidation was not only adsorbed on the electrode surface but also partly distributed in the electrolyte near the electrode surface, while stirring caused this part of elemental sulfur diffused into the electrolyte, reduced the amount of reactant. As a consequence, peak C_1 was weakened to some degree.

The CV curve of pyrite (the second cycle) with the addition of 1×10^{-3} mol/L EDTA in electrolyte is given in Fig. 5. The addition of EDTA shows little influence on oxidation peak A_3 and reduction peak C_1, compared with the CV curve without EDTA. Given the stability constant of EDTA chelating with ferric ion was higher by nearly 10 orders of magnitude than that of ferrous ion, thus, ferric ion was prior chelated by EDTA, according to Nernst equation, the redox potential of the reversible redox couple Fe(III)/Fe(II) would decrease. Actually, it diminished for about 500 mV in the CV curve: peak A_2 shifted from 600 mV to approximately 100 mV and became superimposed on the oxidation peak A_1 of hydrogen sulfide, forming a wide peak, A_1^*; the C_3 shifted from 400 to -100 mV, forming a new peak, C_3^*. EDTA combined with Fe^{2+} generated in Reaction (4) and decreased the concentration of reaction product, and the decrease in product concentration would speed up the reaction. Thus, the ferrous sulfide produced in Reaction (3) would be dissolved more quickly due to the combination of Fe^{2+} with EDTA, which decreased the coverage of ferrous sulfide, and benefited the reduction of pyrite. Consequently, peak C_2 was enhanced, and more hydrogen sulfide was generated. After that, peak A_1, the oxidation of hydrogen sulfide, was also enhanced.

The CV curves of pyrite in electrolyte with other NaCl concentrations were similar to that with 2 mol/L. Through CV studies, we confirmed that the addition of EDTA successfully decreased the potential of redox couple Fe(III)/Fe(II), making Fe(II) being oxidized to Fe(III) at a more negative potential before pyrite oxidation begins. In this way, the adding of EDTA ensures that the iron in oxidation products exists only in the form of Fe(III); the anodic half reaction of pyrite happened as described in Reaction (1).

Table 1 Electrochemical parameters of pyrite anodic polarization under different NaCl concentrations (10^{-3} mol/L EDTA, 1 mV·s^{-1}, pH 3.00)

c_{NaCl} (mol/L)	E_{corr} (mV)	β_a (mV·decade^{-1})	$j_{0,a}$ (mA·cm^{-2})
0	264.5	74.6	6.1×10^{-5}
0.5	207.1	71.2	1.4×10^{-4}
1.0	162.4	69.9	3.8×10^{-4}
1.5	114.3	68.9	5.2×10^{-4}
2.0	91.6	65.8	9.0×10^{-4}

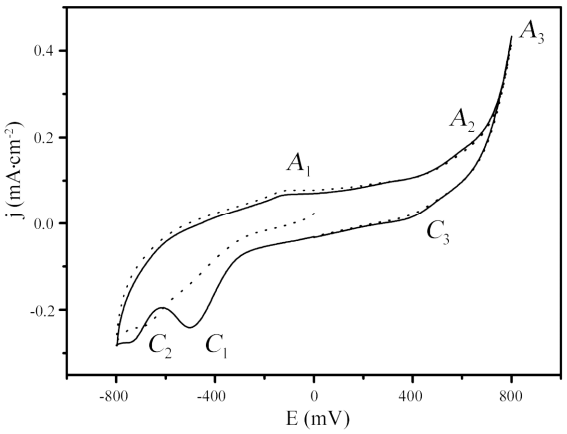

Fig. 3. CV curve of pyrite in 2 mol/L NaCl and 0.1 mol/L $NaClO_4$. Dashed line: first cycle, continuous line: second cycle (scan rate 30 mV·s^{-1}, pH 3.00, without stirring, vs. SCE).

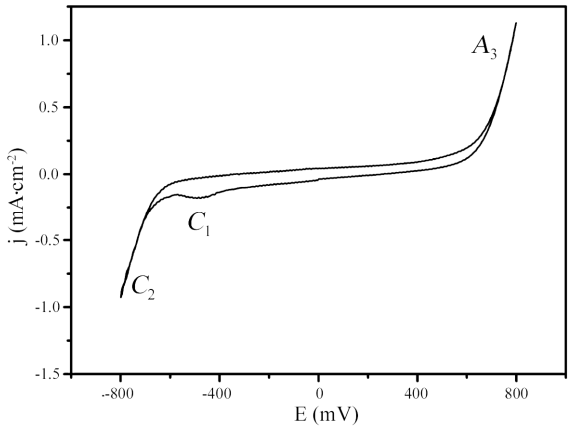

Fig. 4. Second cycle of the CV curve of pyrite in 2 mol/L NaCl and 0.1 mol/L $NaClO_4$ (scan rate 30 mV·s^{-1}, pH 3.00, stirring, vs. SCE).

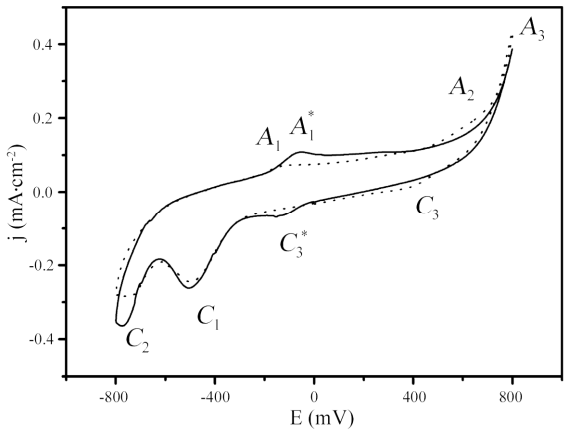

Fig. 5. Second cycle of CV curve of pyrite in 2 mol/L NaCl and 0.1 mol/L $NaClO_4$. Dashed line: without EDTA, continuous line: with 10^{-3} mol/L EDTA (scan rate 30 mV·s^{-1}, pH 3.00, without stirring, vs. SCE).

3.4 Chronoamperometric experiment

Chronoamperometry was used to estimate the dissolution rate of pyrite in solutions with different NaCl concentrations at different potentials (600, 800, and 1000 mV). Iron concentration in the electrolyte was measured by AAS after the reaction.

Fig. 6 showed the current-time curve (without stirring) within 24 hours as the NaCl concentration increased from 0 to 2 mol/L at the potential of 600 mV. At the initial stage of the reaction, the oxidation current density significantly decreased as sulfur accumulated on the surface of the pyrite electrode. Comparison of the current-time curves at different NaCl concentrations revealed that the oxidation current density increased with increasing NaCl. We speculated that the chloride ions prevented elemental sulfur from being deposited on the surface of the electrode, which blocked the passivation of pyrite.

Linear voltammetric scanning was employed to detect the amount of sulfur deposited on the surface of pyrite at different NaCl concentrations. Firstly, a chronoamperometry test at 600 mV for 1 minute was conducted, and resulted in an oxidized surface. Then, a negative going scan from OCP was conducted with stirring, a reduction peak would appear around -500 mV, which represented the reduction of elemental sulfur (Reaction 2). Fig. 7 showed that peak in electrolyte with different NaCl concentrations. The peak area decreased with increasing NaCl concentrations, meant that a higher NaCl concentration would decrease the amount of elemental sulfur deposited on the pyrite surface.

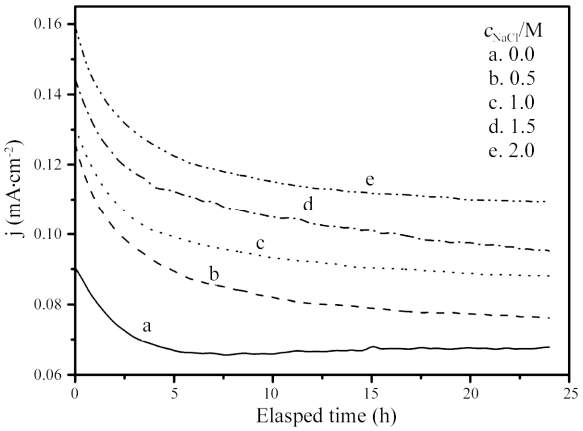

Fig. 6. Chronoamperometric curves of pyrite at 600 mV in electrolyte with different NaCl concentrations (without stirring, pH 3.00, vs. SCE).

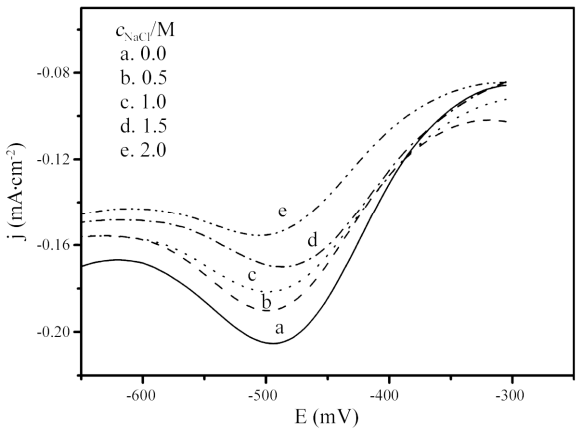

Fig. 7. The reduction peak of elemental sulfur at pyrite surface after 1 minute of chronoamperometric experiment at 600 mV (scan rate 30 mV·s^{-1}, pH 3.00, without stirring, vs. SCE).

Figs. 8 and 9 showed the chronoamperometric curves of pyrite at 800 and 1000 mV for 4 hours (without stirring), respectively. The variation in NaCl concentration in electrolyte was also in the range of 0 – 2 mol/L. As the reaction began, the oxidation current density also decreased with time, but less significantly compared with that at 600 mV. The current-time curves at different NaCl concentrations showed that

the current density decreased with increasing NaCl concentration, which was contrary to the trend at 600 mV. At high potential area, the yield of sulfur decreased, providing less hindering effect on the oxidation rate. Moreover, the electronegative chloride ions would be accumulated on the electrode surface in large quantities under electric field, blocking the pathway by which the water molecules interacted with pyrite (Fig. 10). The steric effect resulted from the absorption of chloride ions would increase the activation energy E_a for pyrite oxidation. Through Arrhenius equation, $k = A\exp(-\frac{Ea}{RT})$, when the activation energy E_a increases, the reaction rate constant k decreases and the reaction rate decreases. Thus, the increasing NaCl concentration in electrolyte hindered the oxidation of pyrite at high potential area.

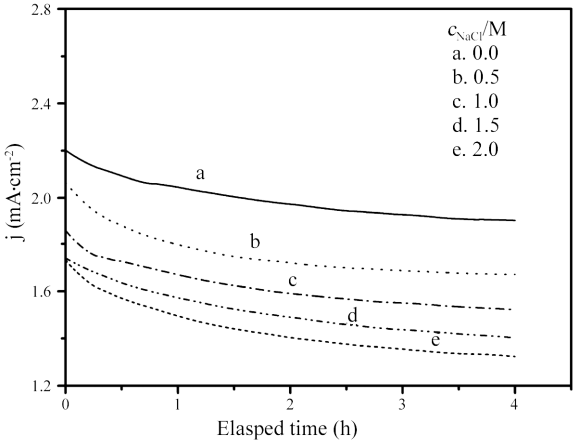

Fig. 8. Chronoamperometric curves of pyrite at 800 mV in electrolyte with different NaCl concentrations (without stirring, pH 3.00, vs. SCE).

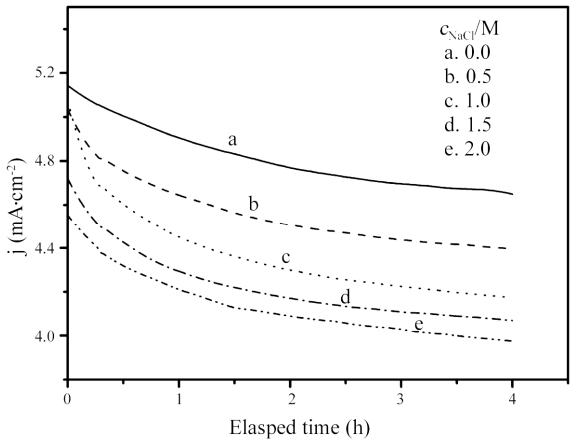

Fig. 9. Chronoamperometric curves of pyrite at 1000 mV in electrolyte with different NaCl concentrations (without stirring, pH 3.00, vs. SCE).

The AAS analysis showed consistent results with chronoamperometry studies (Table 2). The increasing NaCl concentration promoted the oxidation rate of pyrite at 600 mV, while, it decreased the oxidation rate at higher potentials (800 and 1000 mV). The inversion showed the adsorption competition of chloride ions, water molecules and sulfur on pyrite surface. At low potential area, chloride ions are advantage of hindering the adsorption of elemental sulfur, benefiting the reaction between pyrite and water molecules. However, when applied potential increases, chloride ions are adsorbed on the pyrite surface massively by electric field force, blocking the reaction between pyrite and water molecules.

When the environment redox potential (Eh) is lower than 600 mV in pyrite leaching, high chloride ions concentration benefits the oxidation of pyrite not only by the complexation of chloride ions with iron, but also by lessening the passivation of elemental sulfur.

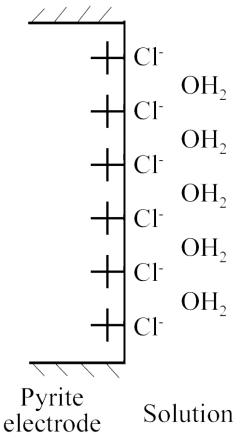

Fig. 10. Double layers formed on the pyrite electrode surface at high potential area.

Table 2 Total charge Q, iron content in electrolyte c_{Fe}^{3+} and x in Chronoamperometric experiments with different NaCl concentrations at 600, 800, and 1000 mV

Potential (mV)	Elapsed time (h)	c_{NaCl} (mol/L)	Q (mC)	$C_{Fe^{3+}}$ (mg·L^{-1})	x
600	24	0.0	5920.80	1.50	0.962
		0.5	7301.44	1.83	0.958
		1.0	8226.28	2.07	0.964
		1.5	9134.16.	2.28	0.962
		2.0	10161.32	2.55	0.961
800	4	0.0	28673.58	5.96	0.640
		0.5	25274.14	5.20	0.618
		1.0	23202.00	4.69	0.592
		1.5	21724.06	4.38	0.576
		2.0	20616.82	4.10	0.568
1000	4	0.0	34638.88	11.37	0.142
		0.5	32806.11	10.64	0.114
		1.0	31274.57	10.10	0.094
		1.5	30257.74	9.67	0.066
		2.0	29612.70	9.39	0.048

3.5 Calculation of the yield of elemental sulfur in chronoamperometric experiment

The amount of elemental sulfur deposited on the surface of pyrite decreased with increasing chloride ion concentration, as indicated by this study and former literatures. However, whether higher chloride ions concentration reduced the production of elemental sulfur or just hindered its deposition on the electrode surface remains unknown. According to Reaction (1) and Faraday's law of electrolysis, $m=\frac{MQ}{nF}$, where m was measured by AAS, whereas the quantity of electric charge Q was derived from the integration of chronoamperometric curves, the number of transferred electron n, (15–6x) in Reaction (1), could be known. Therefore, we could work out the proportion of elemental sulfur in the oxidation products, x/2. Table 2 presents the values of Q and x at different NaCl concentrations and potentials. At 600 mV of potential, the value of x is slightly changed around 0.96 with increasing NaCl concentration. That means that the proportion of elemental sulfur in the oxidation products was barely affected by increasing NaCl concentrations. When the potential increased to 800 and 1000 mV, the value of x decreased with increasing NaCl concentration. At 800 mV of potential, when the NaCl concentration increased from 0 to 2 mol/L, the value of x decreased from 0.640 to 0.568; at 1000 mV, from 0.142 to 0.048. The decreasing x value indicated that chloride ions changed the stoichiometric of pyrite oxidation reaction at higher potential areas. By *in-situ* Raman analysis, Lehmann et al. (2000) found that the presence of chloride ions facilitated the oxidation of intermediate $S_2O_3^{2-}$ to $S_4O_6^{2-}$ and finally SO_4^{2-},

$$2S_2O_3^{2-}\rightarrow S_4O_6^{2-}+2e^- \quad (8)$$

$$S_4O_6^{2-}+2H_2O\rightarrow 2SO_4^{2-}+4H^++2e^- \quad (9)$$

In conclusion, at the potential of 600 mV, the increasing NaCl concentration did reduce the amount of elemental sulfur on pyrite surface; it rarely changed the total amount of elemental sulfur produced in the oxidation. Increasing chloride ion concentration increased the generated elemental sulfur to spread to the electrolyte instead of being adsorbed on electrode surface. However, at 800 and 1000 mV, the proportion of elemental sulfur did decrease with increasing NaCl concentration.

4 Conclusions

(1) The adsorption of chloride ions onto the pyrite surface reduces the threshold energy of the interaction between water molecules with pyrite. When NaCl concentration increased from 0 to 2 mol/L, the OCP dropped from 264.5 to 91.6 mV, β_a decreased from 74.6 to 65.8 mV/decade, and $j_{0,a}$ increased from 6.1×10^{-5} mA·cm^{-2} to 9.0×10^{-4} mA·cm^{-2}. These changes suggest that pyrite oxidation more likely occurred with increasing chloride ion concentration.

(2) At 600 mV, the sulfur adsorbed on pyrite surface accounted for considerable hindering effect on the oxidation rate. The promotion in chloride ion concentrations hindered the adsorption of elemental sulfur, resulting in elevated oxidation rate. The condition at higher potentials (e.g. 800 and 1000 mV) exhibited the reverse, chloride ions accumulated on the pyrite surface, blocking the reaction pathway of pyrite with water molecule. Higher chloride ion concentration reduced the pyrite oxidation rate.

(3) The addition of EDTA reduced the potential of the redox couple Fe(III)/Fe(II) at a scale of approximately 500 mV in the experiment, making the oxidation of Fe(II) to Fe(III) at a more negative potential before pyrite oxidation began. This enabled the calculation of the proportion of elemental sulfur according to Faraday's law of electrolysis even at low potential area. The results showed that the increase in chloride ion concentration rarely changed the proportion of the oxidation products at 600 mV, however, it did reduced the yield of elemental sulfur at higher potentials, at 800 and 1000 mV, the proportions of elemental sulfur in the products reduced from 32% to 28.4% and from 7.1% to 2.4%, respectively.

Acknowledgements This work was financially supported by Large-scale Scientific Apparatus Development Program of Chinese Academy of Sciences (YZ200720), 135 Program of the Institute of Geochemistry, CAS, and Ocean 863 Program (2010AA09Z207) of the Ministry of Science and Technology, China.

References

Ahlberg E. and Broo A.E. (1997) Electrochemical reaction mechanisms at pyrite in acidic perchlorate solutions [J]. *Journal of the Electrochemical Society.* **144**, 1281–1286.

Antonijevic M.M., Dimitrijevic M.D., Serbula S.M., Dimitrijevic V.L.J., Bogdanovic G.D., and Milic S.M. (2005) Influence of inorganic anions on electrochemical behaviour of pyrite [J]. *Electrochimica Acta.* **50**, 4160–4167.

Antonijevic M.M., Dimitrijevic M., and Jankovic Z. (1997) Leaching of pyrite with hydrogen peroxide in sulphuric acid [J]. *Hydrometallurgy*. **46**, 71–83.

Baker B.J. and Banfield J.F. (2003) Microbial communities in acid mine drainage [J]. *FEMS Microbiology Ecology.* **44**, 139–152.

Balci N., Shanks W.C., Mayer B., and Mandernack K.W. (2007) Oxygen

and sulfur isotope systematics of sulfate produced by bacterial and abiotic oxidation of pyrite [J]. *Geochimica et Cosmochimica Acta.* **71**, 3796–3811.

Biegler T. and Swift D.A. (1979) Anodic behaviour of pyrite in acid solutions [J]. *Electrochimica Acta.* **24**, 415–420.

Bonnissel-Gissinger P., Alnot M., and Ehrhardt J.J. (1998) Surface oxidation of pyrite as a function of pH [J]. *Environmental Science and Technology.* **32**, 2845–2869.

Boulton A., Fornasiero D., and Ralston J. (2003) Characterization of sphalerite and pyrite flotation samples by XPS and ToF-SIMS [J]. *International Journal of Mineral Processing.* **70**, 205–219.

Cabral T. and Ignatiadis I. (2001) Mechanistic study of the pyrite–solution interface during the oxidative bacterial dissolution of pyrite (FeS_2) by using electrochemical techniques [J]. *International Journal of Mineral Processing.* **62**, 41–64.

Carneiro M.F.C. and Leao V.A. (2007) The role of sodium chloride on surface of chalcopyrite leached with ferric sulfate [J]. *Hydrometallurgy.* **87**, 73–82.

Chandra A.P. and Gerson A.R. (2009) A review of the fundamental studies of the copper activation mechanisms for selective flotation of the sulfide minerals, sphalerite and pyrite [J]. *Advances in Colloid and Interface Science*. **145**, 97–110.

Chandra A.P. and Gerson A.R. (2011) Redox potential (Eh) and anion effects of pyrite (FeS_2) leaching at pH 1 [J]. *Geochimica et Cosmochimica Acta.* **75**, 6893–6911.

Chernyshova I.V. (2003) An *in-situ* FTIR study of galena and pyrite oxidation in aqueous solution [J]. *Journal of Electroanalytical Chemistry.* **558**, 83–98.

Descostes M., Vitorge P., and Beagucaire C. (2004) Pyrite dissolution in acidic media [J]. *Geochimica et Cosmochimica Acta.* **68**, 4559–4569.

Dutrizac J.E. (1992) The leaching of sulfide minerals in chloride media [J]. *Hydrometallurgy.* **29**, 1–45.

Flatt J.R. and Woods R. (1995) A voltammetric investigation of the oxidation of pyrite in nitric-acid solutions—Relation to treatment of refractory gold ores [J]. *Journal of Applied Electrochemistry.* **25**, 852–856.

Giannetti B.F., Bonilla S.H., Zinola C.F., and Raboczkay T. (2001) A study of the main oxidation products of natural pyrite by voltammetric and photoelectrochemical responses [J]. *Hydrometallurgy.* **60**, 41–53.

Kelsall G.H., Yin Q., Vaughan D.J., England K.E.R., and Brandon N.P. (1999) Electrochemical oxidation of pyrite (FeS_2) in aqueous electrolytes [J]. *Journal of Electroanalytical Chemistry.* **471**, 116–125.

Lehmann M.N., Stichnoth M., Walton D., and Bailey S.I. (2000) The effect of chloride ions on the ambient electrochemistry of pyrite oxidation in acid media [J]. *Journal of the Electrochemical Society.* **147**, 3263–3271.

Lin H.K. and Say W.C. (1999) Study of pyrite oxidation by cyclic voltammetric, impedance spectroscopic and potential step techniques [J]. *Journal of Applied Electrochemistry.* **29**, 987–994.

Liu Yun, Dang Zhi, Wu Pingxiao, Lu Jing, Shu Xiaohua, and Zheng Liuchun (2011) Influence of ferric iron on the electrochemical behavior of pyrite [J]. *Ionics*. **17**, 169–176.

Long H. and Dixon D.G. (2004) Pressure oxidation of pyrite in sulfuric acid media: A kinetic study [J]. *Hydrometallurgy.* **73**, 335–349.

Lowson R.T. (1982) Aqueous oxidation of pyrite by molecular-oxygen [J]. *Chemical Reviews.* **82**, 461–497.

Mckibben M.A. and Barnes H.L. (1986) Oxidation of pyrite in low-temperature acdic solutions—Rate laws and surface textures [J]. *Geochimica et Cosmochimica Acta.* **50**, 1509–1520.

Moses C.O., Nordstrom D.K., and Herman J.S. (1987) Aqeous pyrite oxidation by dissolved-oxygen and by ferric iron [J]. *Geochimica et Cosmochimica Acta.* **51**, 1561–1571.

Moslemi H., Shamsi P., and Habashi F. (2011) Pyrite and pyrrhotite open circuit potentials study: Effects on flotation [J]. *Minerals Engineering.* **24**, 1038–1045.

Rimstidt J.D. and Vaughan D.J. (2003) Pyrite oxidation: A state-of-the-art assessment of the reaction mechanism [J]. *Geochimica et Cosmochimica Acta.* **67**, 873–880.

Senanayake G. (2009) A review of chloride assisted copper sulfide leaching by oxygenated sulfuric acid and mechanistic considerations [J]. *Hydrometallurgy*. **98**, 21–32.

Tao D.P., Richardson P.E., Luttrell G.H., and Yoon R.H. (2003) Electrochemical studies of pyrite oxidation and reduction using freshly-fractured electrodes and rotating ring-disc electrodes [J]. *Electrochimica Acta.* **48**, 3615–3623.

Webera P.A., Stewartb W.A., Skinnera W.M., Weisenera C.G., Thomasa J.E., and Smarta R.S.C. (2004) Geochemical effects of oxidation products and framboidal pyrite oxidation in acid mine drainage prediction techniques [J]. *Applied Geochemistry.* **19**, 1953–1974.

Wei D. and Osseoasare K. (1996) Semiconductor electrochemistry of particulate pyrite: Dissolution via hole and electron pathways [J]. *Journal of the Electrochemical Society.* **143**, 3192–3198.

Williamson M.A. and Rimstidt J.D. (1994) The kinetics and electrochemical rate-determining step of aqueous pyrite oxidation [J]. *Geochimica et Cosmochimica Acta.* **58**, 5443–5454.

Xiong Huixin and Guo Rong (2011) Effects of chloride acclimation on iron oxyhydroxides and cell morphology during cultivation of acidithiobacillus ferrooxidans [J]. *Environmental Science and Technology.* **45**, 235–240.